

Pulsed- Electrochemical Synthesis and Characterizations of Magnetite Nanorods

Hassan Karami^{1,2*}, Elham Chidar¹

¹Department of Chemistry, Payame Noor University, P. O. Box 19395-3697, Tehran, Iran

²Nano Research Laboratory, Department of Chemistry, Payame Noor University, Abhar, Iran

*E-mail: karami_h@yahoo.com

Received: 28 December 2011 / Accepted: 7 February 2012 / Published: 1 March 2012

Magnetite nanorods are synthesized by exerting pulsed current in potassium hydroxide solution for the direct oxidation of iron electrode. The prepared samples are characterized by X-ray diffraction (XRD), scanning electron microscopy (SEM), transmission electron microscopy (TEM), and energy dispersive X-ray (EDX). The effects of synthesis parameters such as pulse height (current amplitude or current density), pulse frequency, solution temperature, potassium hydroxide concentration and type and concentration of synthesis additives on the morphology and particles sizes are investigated by the “one at a time” method. The optimized conditions are 2 M potassium hydroxide, 45°C solution temperature, 18 mA.cm⁻² pulse height, 8 Hz pulse frequency, and 1 g.L⁻¹ cetyltrimethyl ammonium bromide (CTAB) as synthesis director additive conditions to synthesize nanostructured magnetite. In the optimized conditions, nanomagnetite is synthesized in nanorod form with 67 nm average diameter and 900 nm average lengths.

Keywords: Nanomagnetite; Nanorods; Pulsed current, Electrosynthesis

1. INTRODUCTION

Physical and chemical properties of nanoscale particles are very different from the bulk materials [1-3]. This change of behavior is the same for iron oxide [4]. Among the numerous metal oxides, iron oxide (Fe₃O₄; Magnetite) nanoparticles are of intense interest and have been extensively investigated for their applications. Magnetite has been attracting attention in the biomedical applications because of its biocompatibility and low toxicity in the human body [5, 6]. Also magnetite has been used as a catalyst for many reactions of important industrial productions [7-10] such as the

NH₃ production, alcohol oxidation, and Fisher-Tropsch synthesis for hydrocarbons and it can catalyze oxidation/reduction reactions [11]. On the other hand, magnetite was used in pigment and related industries [12]. Iron oxide (magnetite) can also be used in wastewater purification [13]. It can be an absorbent for heavy metal from water [14]. The synthesis of iron oxide nanoparticles of controlled shapes has attracted much attention because the physical and chemical properties depend strongly on particles size and morphology.

During the past several years, the development of reliable, simple and efficient methods for synthesizing large amounts of uniformly sized and novel structured iron oxide nanoparticles has been one of the main goals in chemistry research. Recently several chemical methods are employed to synthesize iron oxide nanoparticles such as sol-gel [15], hydrothermal [16, 17], solid state [18, 19], wet milling [20], pyrolysis [21], and microemulsion [22]. The synthesis method plays a key role in determining the morphology, particles sizes, and shape. On the other hand, the electrochemical methods were used to synthesize different nanostructured materials, such as Palladium [23], SnO₂ [24] and super-hydrophilic polypyrrole [25]. Cyclic voltammetry [26], potentiostatic [27, 28], galvanostatic [29, 30] and pulsed current [31-36] as different electrochemical techniques were used to synthesize nanoparticles. Many reports that show pulsed current routes present a simple, quick, and economical method for the preparation of various types of nanoparticles.

In previous studies, we successfully applied the pulsed current technique to synthesize lead dioxide nanoparticles [32, 33], cadmium sulfide nanofibers [34], cobalt nanorods [35], iron nanoclusters [36], and nickel nanoclusters [37].

In this work, we synthesized iron oxide nanoparticles by the pulsed current electrochemical method on the surfaces of iron-based electrodes immersed in alkaline solution. The pulsed current technique has some advantages such as being nonhazardous and, inexpensive and it is a method considered proper for use in laboratory and industrial applications alike. Nanomagnetite is produced in this method with high purity. The effects of experimental parameters of the synthesis, such as pulse current, pulse frequency, solution temperature, potassium hydroxide concentration and synthesis additives have been studied. The amounts of synthesis parameters were varied to find the optimum conditions to synthesize magnetite nanorods. The techniques of SEM, TEM, EDX, and XRD were used to investigate the morphology, the particles sizes, and the composition of the prepared iron oxide samples.

2. EXPERIMENTAL

2.1. Materials

Potassium hydroxide (KOH) was purchased from Merck and used without any purification. Sodium dodecyle sulfate (SDS), triton X-100, cetyl trimethyl ammonium bromide (CTAB), polyvinyl pyrrolidone (PVA), saccharine and glycerol with high purity were obtained from Loba Chimie (India). Double-distilled water was used in all experiments.

2.2. Instrumentals

The morphology and the particles sizes of the iron oxide samples were studied by a Philips scanning electron microscopy (XL30 model). A Philips X'Pert diffractometer with Cu ($K\alpha$) radiation ($\lambda = 0.15418$ nm) was used to study the phase composition and the particles sizes of iron oxide samples. The constant current was supplied by an MPS-3010L model of power source (Taiwan Matrix Co.). A home-made electrical pulse apparatus was used to create the consistently current pulses. The temperature of the synthesis solutions was kept constant by a water bath (Pars Azma Co., Iran).

2.3. Procedure

First, the iron electrodes were put in concentrated nitric acid for 1 min, then twice rinsed with distilled water to clean any surface pollutant. An electrochemical cell containing three iron electrodes (two cathodes and one anode) was immersed in potassium hydroxide solution. The different amounts of pulse currents were exerted into this cell to oxidize iron anode into iron oxide nanoparticles for 24 h. The prepared particles were then collected by a paper filter and dried at 400°C for 2 h. The effects of different parameters, such as reaction temperature, pulse current, pulse frequency, potassium hydroxide concentration and type and concentration of different additives, were optimized by the "one at a time" method to obtain uniform nanorods.

3. RESULT AND DISCUSSION

Iron substrate was used as the initial material to be converted into iron oxide. First, the used iron electrode was analyzed by Energy Dispersive X-ray (EDX) to verify its acceptable purity. Figure 1 shows the EDX patterns.

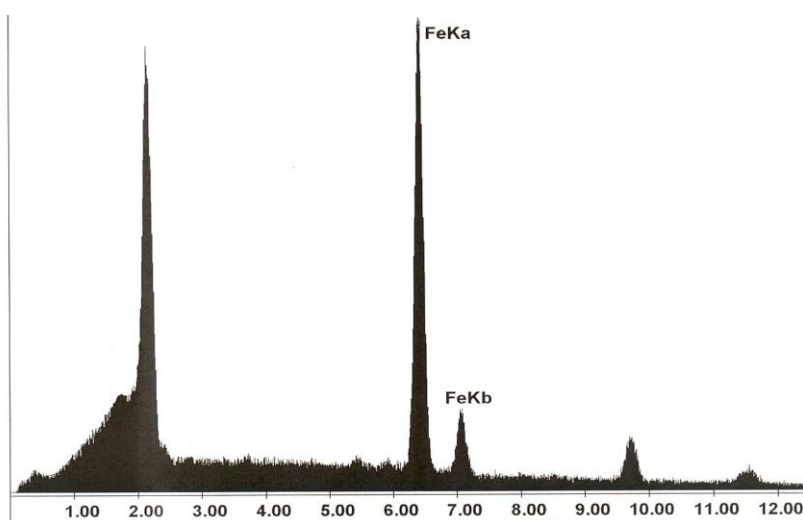


Figure 1. EDX patterns for the iron oxide sample that synthesized at a pulse height of $3\text{mA}\cdot\text{cm}^{-2}$, pulse frequency of 8 Hz, solution temperature of 25°C and 4 M potassium hydroxide concentration

Based on the data shown in Fig. 1, the iron substrate has only Mn (1.86 %wt) and Cr (1.49 %wt) as impurities. Chemical specifications of Mn, Cr and Fe reveal that Fe is oxidized before Cr and Mn. Therefore, during controlled oxidation of iron, Mn and Cr have no interference.

During the synthesis process, direct current with stable amplitude was provided by a common power supply instrument. The output of power the supply system was connected to the home-made pulse maker. The output current of the pulse system is a dc pulse. In the present method, each pulse cycle contains one pulse time (T_{on}) and one relaxation time (T_{off}). Pulse frequency is the number of pulse cycles applied in a time unit (1 s). Figure 2 shows the used pulse diagram and its parameters.

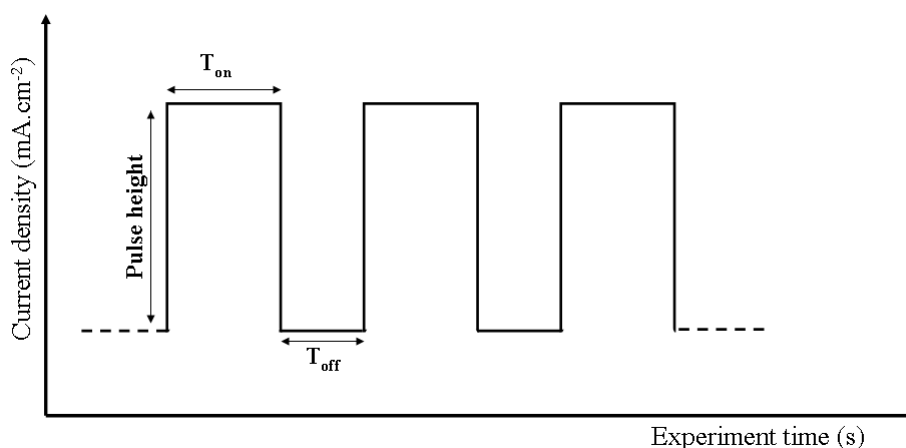


Figure 2. Pulse diagram used for synthesizing iron oxide nanostructures

The pulsed current technique has four instrumental variables including pulse time (t_{on}), relaxation time (t_{off}), pulse height and pulse frequency. Based on previous studies [32-37], the t_{off}/t_{on} ratio of 3 is suitable to synthesize metal oxide nanoparticles. Therefore in this study, we used this ratio, but the other pulse parameters including pulse height, pulse frequency and pulse time were optimized in this work. Besides pulse parameters, the effects of chemical parameters, including concentrations of potassium hydroxide and synthesis additives and synthesis temperatures were studied on the morphology, the particles sizes and the composition of the samples. In the following sections, the optimization experiments and the obtained results will be discussed.

3.1. Effect of pulse height

In the present method, pulsed current with constant amount of current during exerting the pulse into the electrochemical cell is used to direct oxidation of iron substrate. During exerting the current pulse into the system, cell voltage can increase from zero up to a final value. The cell voltage depends on three factors including cell temperature, solution conductivity and the distance between anode and cathode. In a typical experiment according to the section 2.3, the cell voltage can increase from zero up to 12 V.

In the first experiment, the effects of pulse height were evaluated on the synthesis of iron oxide nanoparticles. The amount of height varied from 3 to 200 mA.cm⁻², but the amounts of other parameters were constant (temperature 25°C, pulse frequency 8 Hz and potassium hydroxide concentration 4M). Figure 3 shows the morphology and particles sizes of the synthesized samples.

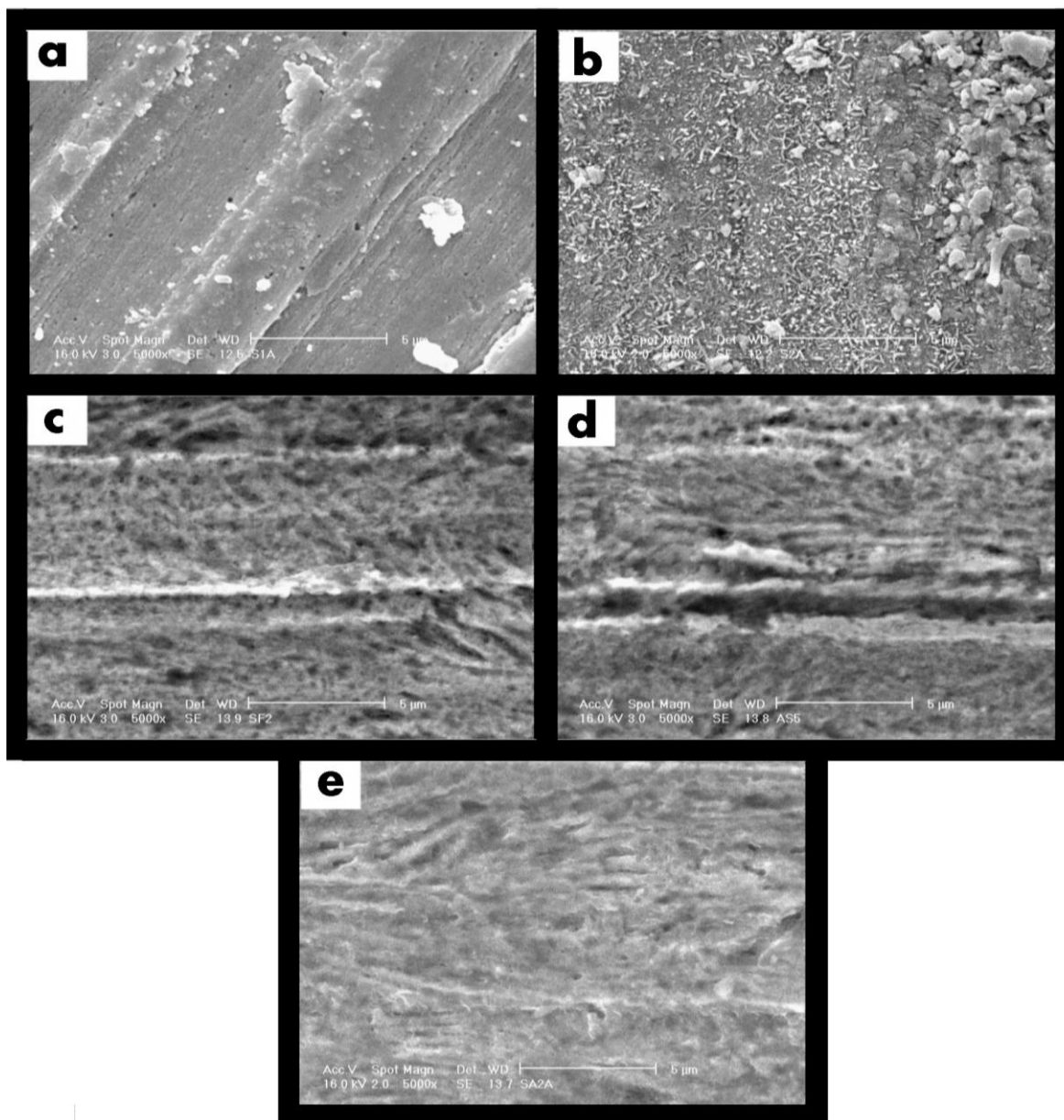


Figure 3. SEM images of the iron oxide samples that synthesized at different current densities, namely, 3 mA.cm⁻² (a), 18 mA.cm⁻² (b), 100 mA.cm⁻² (c), 150 mA.cm⁻² (d) and 200 mA.cm⁻² (e).

Figure 3 shows that, the pulse current of 18 mA.cm⁻² causes the formation of uniform and organized particles with respect to the other currents. In pulse current of 3 mA.cm⁻², the synthesis rate was very slow; thus the total time of synthesis was very long. By using 3 mA.cm⁻², we synthesized an

amorphous sample with low porosity. The porosity of samples is increased by increasing pulsed-current density (pulse height) of up to $18 \text{ mA}\cdot\text{cm}^{-2}$. At this density, magnetite nanorods start to form. Because of greater nucleation rate at higher currents, all nanoparticles were agglomerated. Also, no nanorods appeared in the samples that synthesized at higher current densities. Therefore $18 \text{ mA}\cdot\text{cm}^{-2}$ was selected as the optimum current density (pulse height) for further studies.

There are many reports about the growth mechanisms of magnetite nanorods that synthesized by the non-electrochemical methods [38-41]. The growth mechanism of magnetite nanorods in pulsed-electrochemical synthesis is probable different than those of previous reported methods such as anisotropic growth. In the pulsed current synthesis, particle growth is slow so that magnetic properties of an initial magnetite seed formed on the surface of the electrode induce a controlled direction to joint the next produced magnetite species (iron and oxygen ions) until formation of a nanorod.

3.2. Effect of pulse frequency

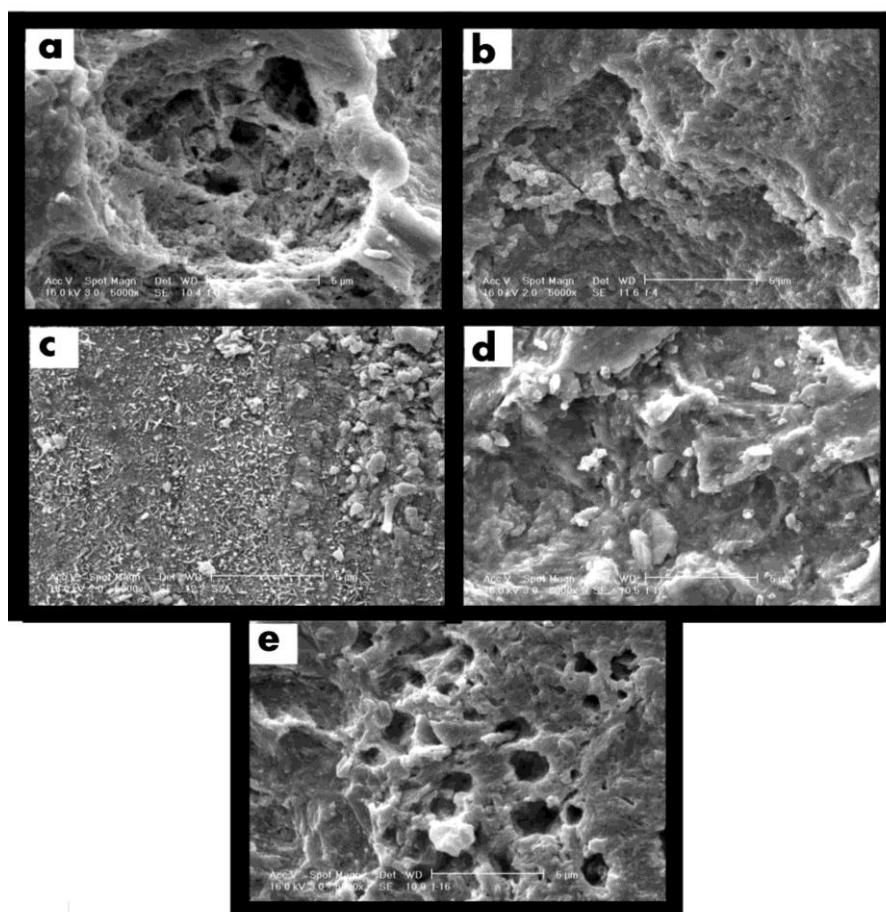


Figure 4. SEM images of the samples that synthesized at different pulse frequencies; (a) simple constant current, (b) 6 Hz, (c) 8 Hz, (d) 14 Hz, and (e) 16 Hz.

The effects of pulse frequency were studied on the morphology and the particles sizes of iron oxide nanoparticles. The amount of pulse frequency varied from 0 to 16 Hz, but the other parameters

were constant (temperature 25 °C, pulse height 18 mA.cm², and potassium hydroxide concentration 4M). Figure 4 shows the SEM images of iron oxide (magnetite) samples that synthesized at different pulse frequencies.

It is obvious from Fig 4a that constant current (pulse frequency of 0) is not suitable to synthesize iron oxide nanostructures. By using pulsed current, we converted the amorphous and agglomerated samples to the nanostructured sample (Fig. 4b and 4c). At frequency of 8 Hz, the agglomeration of iron oxide particles was decreased and the particles changed to needle shape nanorods. At the higher frequencies (12 Hz: Fig. 4d; 16 Hz: Fig. 4e), the iron oxide particles are transferred to agglomerated and amorphous powder because the relaxation time between two consequent pulses is very low; thus before the particle formation in the first pulse is completed, the next pulse will be applied. This phenomenon causes large agglomerated particles to form.

The obtained results showed that the pulsed-current technique can control the morphology of the sample. The frequency of 8 Hz was chosen as an optimum pulse frequency for the electrosynthesis of iron oxide nanoparticles.

3.3. Electrosynthesis temperature

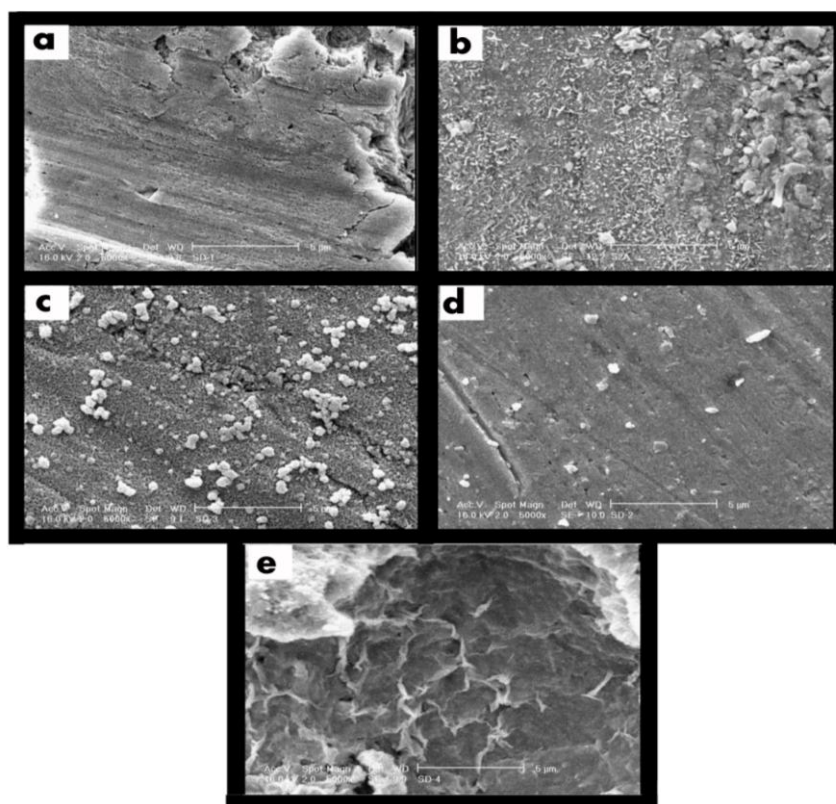


Figure 5. SEM images of the iron oxide samples synthesized at different temperatures; (a) 0°C, (b) 25°C, (c) 45°C and (d) 75°C. Nanomagnetite and nanohematite peaks were marked by 1 and 2, respectively.

Based on our previous studies [32-37], the temperature of electrosynthesis solution is an important parameter that can affect the morphology, the particles sizes, and the composition of the

final yield. The synthesized samples at different temperatures were characterized by SEM and XRD. The SEM images shown in Fig. 5 present the effects of synthesis temperature on the morphology and particles sizes of magnetite samples.

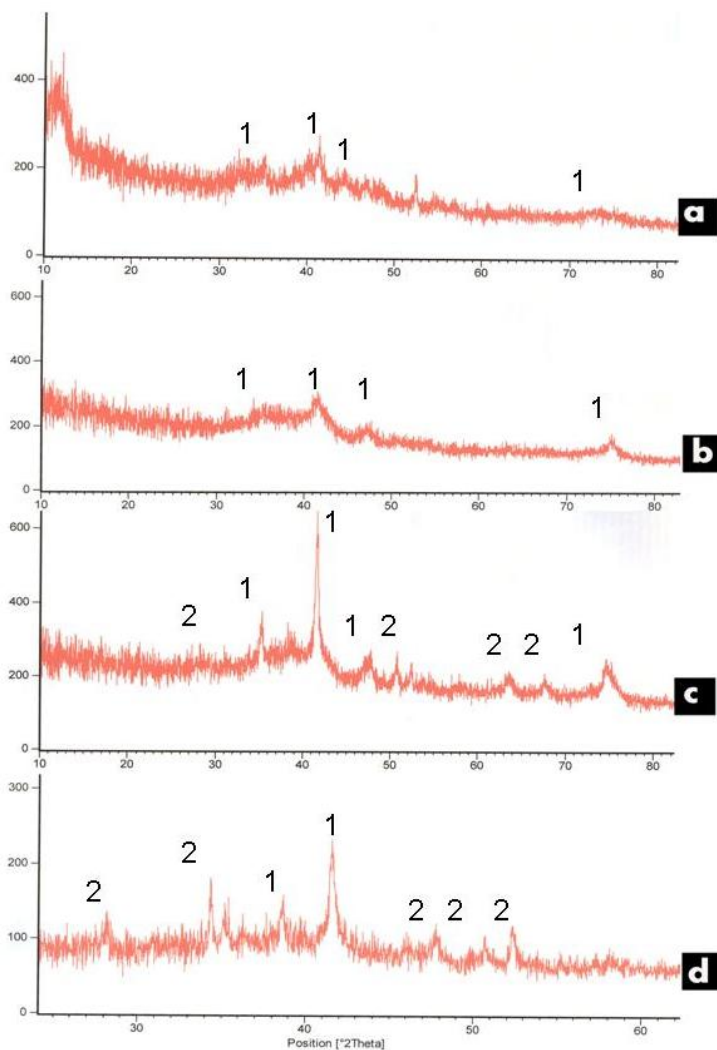
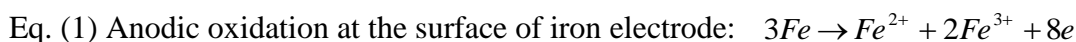


Figure 6. XRD patterns of the iron oxide samples synthesized at different temperatures; (a) 0°C, (b) 25°C, (c) 45°C and (d) 75°C. Nanomagnetite and nanohematite peaks were marked by 1 and 2, respectively.

Based on the SEM images shown in Fig. 5, the sample morphology was converted from agglomerated spherical nanoparticles into nanorods when the synthesis temperature was increased to 46°C, from 0°C. The effects of temperature can be related to rate constants of two nucleation and particle growth processes. At higher temperatures (>45°C), agglomeration and changing of morphology into spherical nanoparticles were observed. By comparing the SEM images, the synthesis temperature of 45 °C makes the most uniform and smallest nanorods. Therefore this temperature can be selected for further studies, but the XRD patterns of the synthesized samples at different temperatures make it necessary to change this selection.

Figure 6 shows the effect of synthesis temperature on the XRD patterns. Based on the XRD results, the sample synthesized at 25°C or lower contains only Fe₃O₄ (magnetite). At higher temperatures, it contains Fe₃O₄ (magnetite) and α-Fe₂O₃ (hematite). The oxidation state of iron increases when the synthesis temperature is increased so that at a higher temperature, iron can oxidize to Fe³⁺ to form hematite. With respect to SEM images and XRD patterns, 25°C is suitable to synthesize pure nanomagnetite.

The effect of temperature can be explained by considering the following reactions:



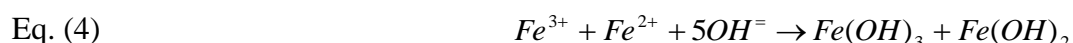
At low temperatures (below 45°C), iron substrate is oxidized to Fe³⁺ and Fe²⁺ with ratio 2:1 (Eq. 1). Fe³⁺ and Fe²⁺ ions converted into nanomagnetite according to Eq. 2. At higher temperatures (above 45°C), the Fe³⁺ content exceeds the 2:1 ratio. The Fe³⁺ excess is converted into nanohematite (Fe₂O₃). Therefore the synthesized samples at higher temperatures (45°C and more) include a mixture of nanomagnetite and nanohematite.

3.4. Effects of potassium hydroxide concentration

Potassium hydroxide concentration is a most- important factor in the proposed synthesis. Six samples were synthesized in the solution containing 0.5, 1, 2, 3, 4 and 5 M potassium hydroxide to evaluate the effect of this factor on the morphology and particles sizes of magnetite samples. The synthesized samples were studied by SEM.

Figure 7 shows the SEM images of the samples. It can be seen in Fig. 7 that the morphologies of samples change from irregular nanoparticles into uniform nanorods, when the hydroxide concentration increases to 2 M from 0.5 M. At higher concentrations (more than 2 M), the samples are strongly agglomerated and changed to amorphous sample.

The formation reactions for nanomagnetite and nanohematite have been presented in Eqs 2 and 3. At higher concentrations of hydroxide ion, the following reaction is carried out:



Iron hydroxide species are seen as amorphous form in Figs 7e and 7f. Based on the presented results, the 2 M potassium hydroxide solution is the best electrolyte to synthesize nanostructured magnetite.

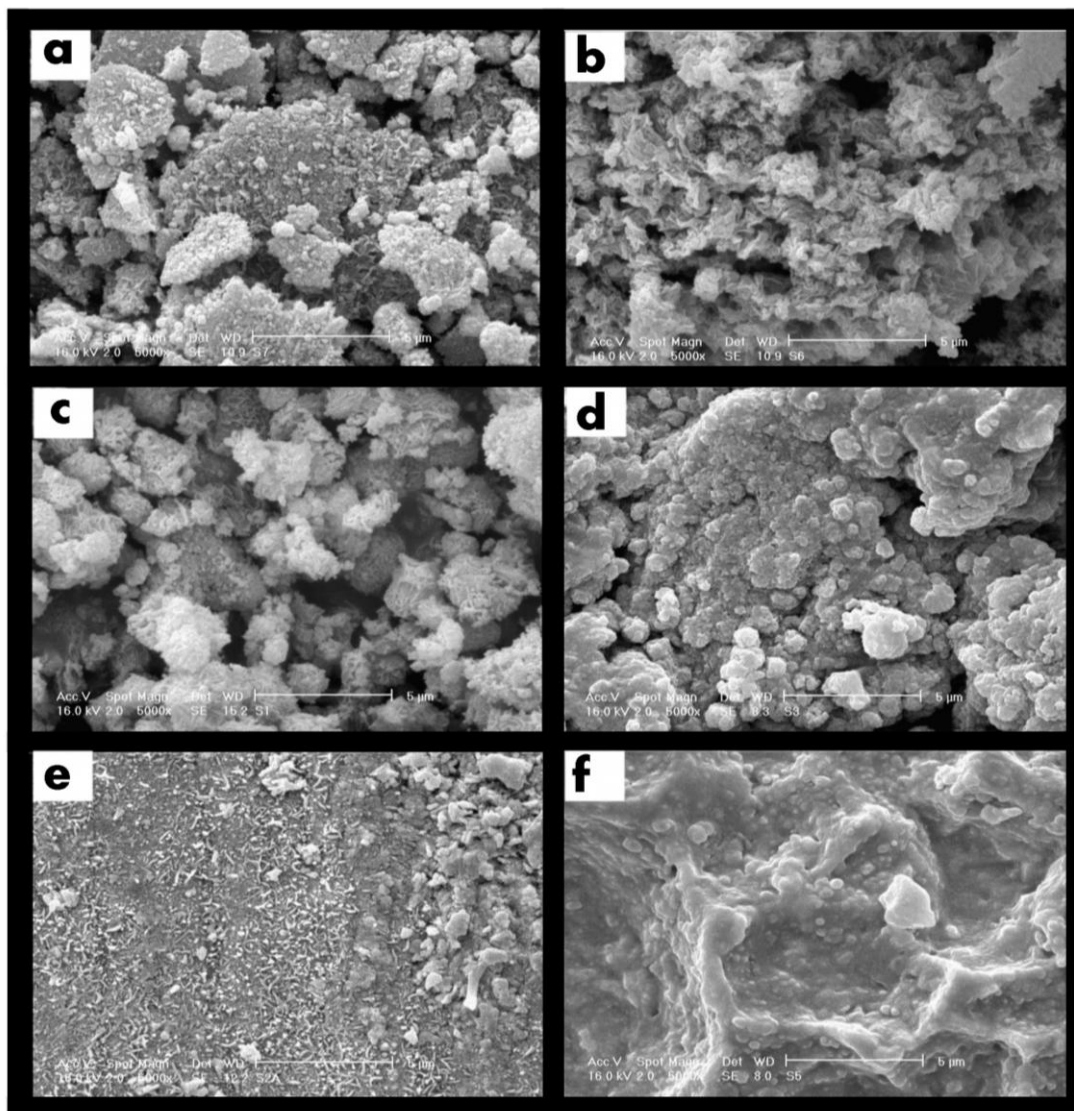


Figure 7. SEM images of the samples synthesized at different hydroxide concentrations; 0.5 M (a), 1 M (b), 2 M (c), 3 M (d), 4 M (e), and 5 M (f).

3.5. Effects of synthesis additives

Surfactants are used as director agents to control the mechanism and kinetics of the reactions in synthesis processes of nanomaterials. These additives can affect the morphology and particles sizes of the final product [42]. The sizes distribution of the nanoparticles can be controlled by adding a surfactant [43]. Different surfactants have been employed in the synthesizing of nanoparticles such as bis(2-ethylhexyl) sulfosuccinate (AOT), sodium dodecyl sulfate (SDS), cetyltrimethyl ammonium bromide (CTAB), polyvinyl pyrrolidone (PVP) and diethyl sulfosuccinate (DES) [44-46]. In this study, the effect of PVP, saccharin, SDS, glycerol, CTAB and triton X-114 was investigated on the morphology and particles sizes of iron oxide nanoparticles.

For a selection of suitable additives, several synthesizes were carried out in the presence of different additives with the same concentration (5 g.L^{-1}). Initial experiments showed that PVP, SDS

and glycerol are not suitable as additives in magnetite electrosynthesis. These additives are made to extremely decrease the rate of nanomagnetite synthesis. Figure 8 shows the SEM images of the samples synthesized in the presence of saccharin, CTAB, and triton X-114 as synthesis additives.

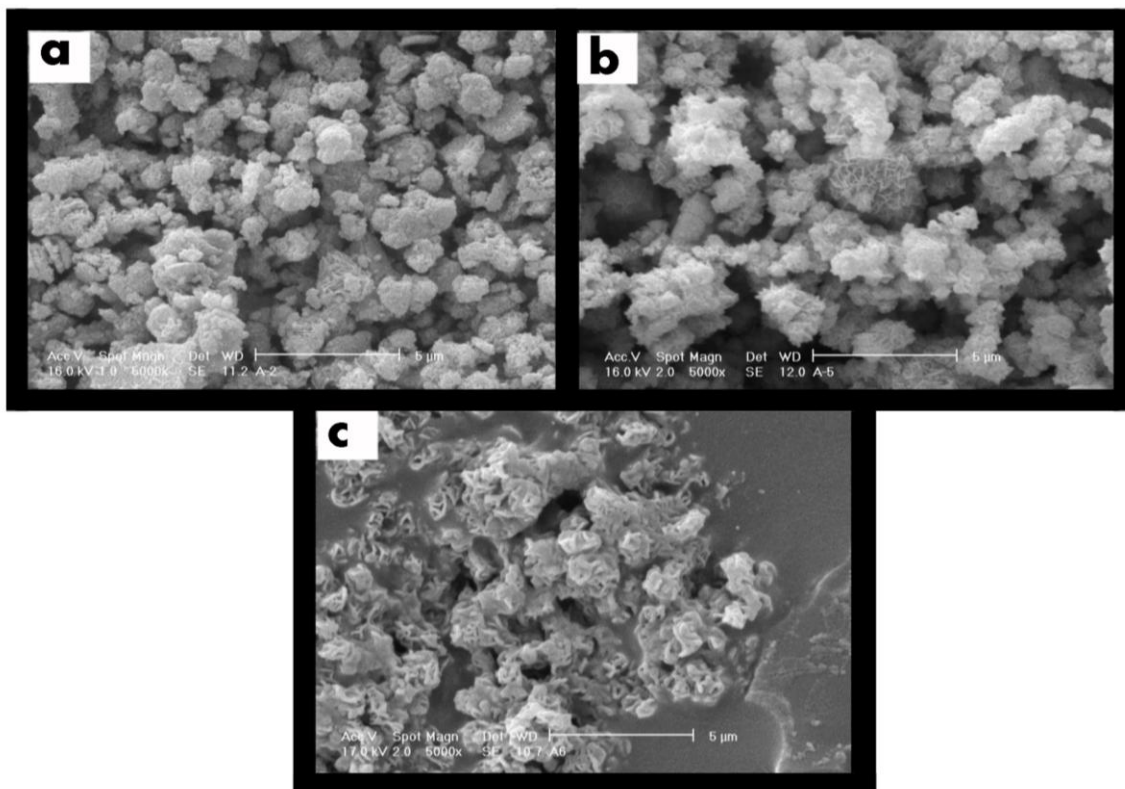


Figure 8. Effects of saccharin (a), CTAB (b) and triton X-114 (c) on the morphology of nanomagnetite samples. Each additive has been used in 5 g.L^{-1} .

As Fig. 8 shows, CTAB acts better than the others. In the presence of CTAB, the sample includes uniform nanorods. At the next step, the effects of CTAB concentration were studied on the sample morphology (Fig. 9).

As Fig. 9 shows, by using 1 g.L^{-1} CTAB in 2 M potassium hydroxide solution, a sample containing uniform nanorods can be synthesized. Therefore 1 g.L^{-1} CTAB is suitable to control the formation of magnetite nanorods. CTAB in 2 M potassium hydroxide solution converts homogeneously into cetyltrimethyl amine and potassium chloride. The formed cetyltrimethyl amine acts as a suitable complex agent to stabilize iron ions (Fe^{2+} and Fe^{3+}). The complex formation can change kinetics and the mechanism of a magnetite formation.

Based on the results, optimized conditions to synthesize magnetite nanorods follow:

Potassium hydroxide: 2 M

Pulsed current amplitude: 18 mA.cm^{-2}

Pulse frequency: 8 Hz

CTAB concentration as synthesis director (additive): 1 g.L^{-1}

Figure 10 shows the SEM image and TEM images of the magnetite nanorods synthesized at the optimum conditions mentioned above. Because it is visible in Fig. 10, the optimized sample includes uniform nanorods with 67 nm average diameter and 900 nm average lengths.

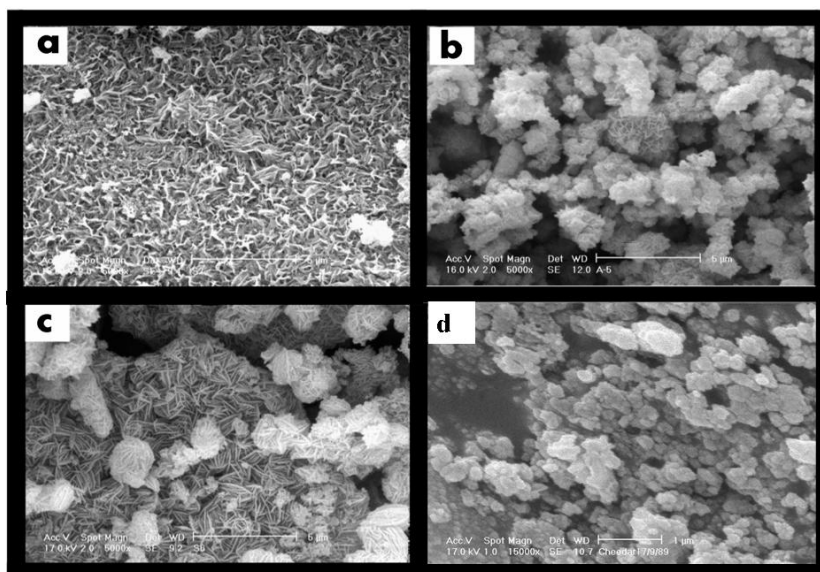


Figure 9. SEM images of the samples synthesized at different concentrations of CTAB; 3 g.L⁻¹ (a), 2 g.L⁻¹ (b), 1 g.L⁻¹ (c) and 0.5 g.L⁻¹ (d).

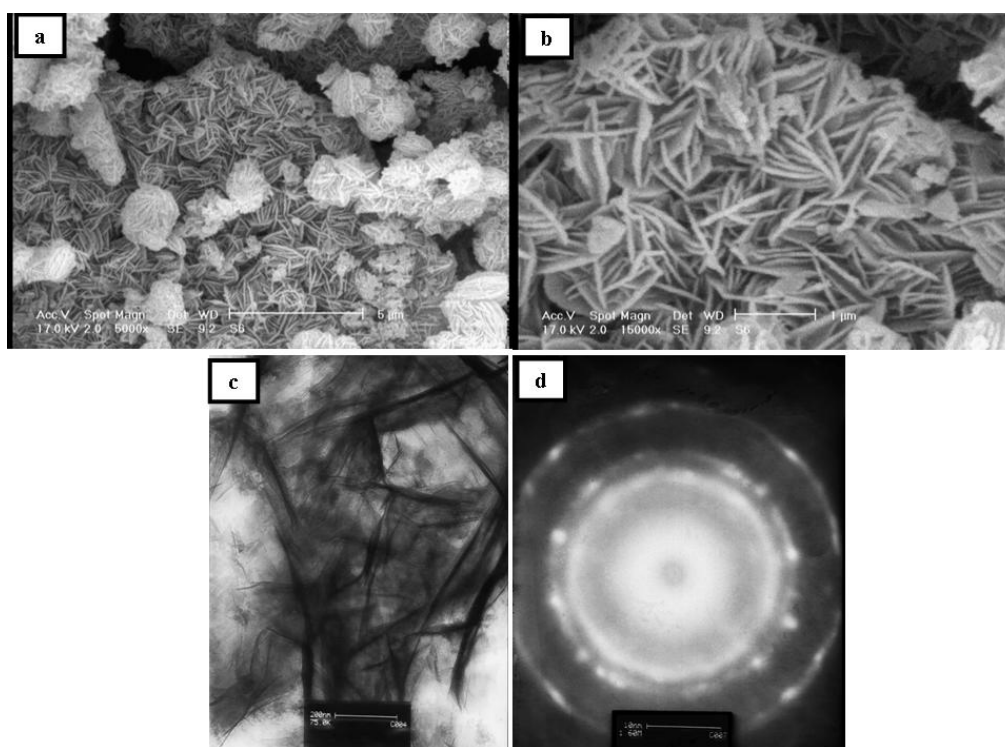


Figure 10. SEM images with different magnifications (a: 5000X and b: 15000X) and TEM images (c and d) of the optimized magnetite nanorods

4. CONCLUSIONS

Magnetite nanorods can be prepared by using a pulsed-current electrochemical method. In this method, pulse height (pulsed current amplitude), pulse frequency, electrolyte concentration, solution temperature and synthesis additive are effective parameters that can change the morphology, the particles sizes, and the composition of samples. By using suitable amounts for the effective parameters, we can synthesize pure magnetite in uniform nanorods. The solution temperature is a most important parameter that can change a sample composition from magnetite to a magnetite and hematite mixture. CTAB is a suitable additive to control the magnetite morphology. The experimental results showed that the pulsed current method is a confident and controllable method to synthesize metal oxide nanoparticles.

ACKNOWLEDGMENT

We gratefully acknowledge the support of this work by Payame Noor University Research Council (Abhar Branch).

References

1. J. Kreuter, *J. Anat.* 189 (1996) 503-505.
2. S. Nair, A. Sasidharan, V. V. D. Rani, D. Menon, S. Nair, K. Manzoor and S. Raina, *J Mater. Sci: Mater Med* 20 (2009) 235-241.
3. R. D. Norman, R. W. Phillips, M. L. Swartz and T. Frankiewicz, *J. Dent. Res.* 43 (1964) 252-262.
4. J. Chatterjee, Y. Haik and C. J. Chen, *J. Magnet. Magnet. Mater.*, 257 (2003) 113-118.
5. P. Majewski and B. Thierry, *Crit. Rev. Solid State Mater. Sci.* 32 (2007) 203-215.
6. P. Tartaj, M. P. Morales, T. Gonzalez-Carreno, S. Veintemillas-Verdaguer and C. J. Serna, *J. Magnet. Magnet. Mater.* 28 (2005) 290-291.
7. M. Azhar Uddin, H. Tsuda, S. Wu and E. Sasaoka, *Fuel* 87 (2008) 451-459.
8. C. Li, Y. Shen, M. Jia, S. Sheng, M. O. Adebajo and H. Zhu, *Catal. Commun.* 9 (2008) 355-361.
9. F. Shi, M. K. Tse, M. M. Pohl, A. Bruckner, S. M. Zhang and M. Beller, *Ange. Chem.* 46 (2007) 8866-8868.
10. C. T. Wang and R. J. Willey, *J. Non-Crystal. Solids* 225 (1998) 173-177.
11. Q. Liu, Z. M. Cui, Z. Ma, S. W. Bian, W. G. Song and L. J. Wan, *Nanotech.* 118 (2007) 37-45.
12. J. H. Meg, G. Q. Yang, L. M. Yan and X. Y. Wang, *J. Dyes Pigments* 66 (2005) 109-115.
13. D. Mohan and C. U. Pihman, *J. Hazard. Mater.*, 142 (2007) 1-53.
14. D. Mohan and C. U. Pittmang, *J. Hazard. Mater.*, 137 (2006) 762-811.
15. N. J. Tang, W. Zhang, H. Y. Jiang, X. L. Wu, W. Lio and Y. W. Du, *J. Magnet. Magnet. Mater.*, 282 (2004) 92-95.
16. S. Ni, X. Wang, G. Zhou, F. Yang, J. Wang, Q. Wang and D. He, *J. Mater. Letter* 63 (2009) 2701-2703.
17. K. He, C. Y. Xu, L. Zhen and W. Z. Shao, *J. Mater. letter* 61 (2007) 3159-3162.
18. A. Ljinas, R. Brucas, V. Stankus and J. Dudonis, *J. Mater. Sci. Eng.* 25 (2005) 586-590.
19. H. Karami, *J. Clust Sci.*, 21 (2010) 11-20.
20. D. Chen, S. Ni and Z. Chen, *J. China Particuology* 5 (2007) 357-358.
21. W. S. Chiu, S. Radiman, M. H. Abdullah, P. S. Khiew, N. M. Huang and R. A. Shukor, *J. Mater. Chem. Phys.* 106 (2007) 231-235.
22. A. B. Chin and I. I. Yaacob, *J. Mater. Proces. Tech.* 191 (2007) 235-237.

23. R. A. Khaydarov, R. R. Khaydarov, O. Gapurova, Y. Estrin and T. Scheper, *J. Nanopart Res* 11 (2009)1193-1200.
24. M. Lai, J. H. Lim, S. Mubeen, Y. Rheem, A. Mulchandani and M. A. Deshusses, *J. Nanotech.* 20 (2009) 185602-18607.
25. K. L. Chen, C. J. Huang, P. H. Chiu and Y. H. Wang, *J. Key Eng. Mater.* 435 (2010) 434-440.
26. H. Karami, A. Yaghoobi and A. Ramezani, *Int. J. Electrochem.Sci.* 5 (2010) 1046-1059.
27. T. Gao, G. Meng, Y. Wang, S. Sun and L. Zhang, *J. Phys.: Condens. Matter* 14 (2002) 355-360.
28. M. Mazur, *J. Electrochem. Commun.* 6 (2004) 400-403.
29. X. H. Lu, W. X. Zhao, G. R. Li, H. Hong and Y. Tong, *J. Mater. Lett.* 62 (2008) 4280-4285.
30. J. Zhang , L. B. Kong , H. Li, Y. C. Luo , L. Kang, *J. Mater. Sci.* 45 (2010) 1947-1954.
31. I. J. Shon, H. K. Park, K. S. Nam and K. T. Lee, *J. Ceramic process Res.* 9 (2008) 325-329.
32. H. Karami and M. Alipour, *Int. J. Electrochem. Sci.* 4 (2009) 1511-1527.
33. H. Karami, B. Kafi and S. N. Mortazavi, *Int. J. Electrochem. Sci.* 4 (2009) 414-424.
34. H. Karami and A. Kaboli, *Int. J. Electrochem. Sci.* 5 (2010) 706-719.
35. H. Karami and E. Mohammadzadeh, *Int. J. Electrochem. Sci.* 5 (2010) 1032-1045.
36. H. Karami, O. Rostami-Ostadkalayeh, *J. Clust. Sci.* 20 (2009) 587-600.
37. H. Karami and S. Mohammadi, *J. Clust. Sci.* 21 (2010) 739-752.
38. S. Chen, J. Feng, X. Guo, J. Hong and W. Ding, *Mater. Lett.* 59 (2005) 985-988.
39. F. Cao, C. Chen, Q. Wang and Q. Chen, *Carbon* 45 (2007) 727-731.
40. J. Wang, Z. Peng, Y. Huang and Q. Chen, *J. Crys. Growth* 263 (2004) 616-619.
41. J. Yue, X. Jiang and A. Yu, *J. Nanopart. Res.* 13 (2011) 3961-3974.
42. G. Lelong, S. Bhattacharyya, S.Kline, T. Cacciaguerra, M. A. Gonzalez and M. L. Saboungi, *J. Phys. Chem. C* 112 (2008) 10674-10680.
43. J. Lee, T. Isobe and M. Senna, *Colloid Interface Sci.* 177 (1996) 490-494.
44. C. W. Kwon, T. S. Yoon, S. S. Yim, S. H. Park and K. B. Kim, *J. Nanopart. Res.* 11 (2009) 831-839.
45. Y. Köseoğlu, *J. Magnet. Magnet. Mater.* 300 (2006) 327-330.
46. Z. Y. Yuan, T. Re and B. L. Su, *Catalysis Today* 95 (2004) 743-750.